CONTRIBUTION OF UREA-N TO NITRIFICATION IN THE SOUTHERN OCEAN

WEST OF THE ANTARCTIC PENINSULA

J T. Hollibaugh^{a,#}; A. Okotie-Oyekan^{a,*}, J. Damashek^{a,†}; H. Ducklow^b,

B. N. Popp^c; N. Wallsgrove^c and T. Allen^c

Department of Marine Sciences, University of Georgia, Athens, GA, USA

^bLamont-Doherty Earth Observatory, Columbia University, Palisades NY, USA

^cDepartment of Earth Sciences, University of Hawai'i at Manoa, Honolulu, HI, USA

#Corresponding author: James Hollibaugh (aquadoc@uga.edu) ORCID: 0000-0001-8037-160X

*Present address: Environmental Studies Program, University of Oregon, Eugene, OR, USA

[†]Department of Biology, Utica College, Utica, NY, USA

DRAFT: 22 April 2023

FOR SUBMISSION TO: Applied and Environmental Microbiology

RUNNING TITLE: Southern Ocean nitrification

KEYWORDS: Thaumarchaeota, nitrification, ammonia-oxidation, urea, *ureC*, *amoA*,

Nitrospina, Antarctica, PAL-LTER, Southern-Ocean Hollibaugh et al. (2023) Main Text

Page 1 of 42

NOTE: THIS MS IS TO BE SUBMITTED FOLLOWING OUTCOME OF NATURE COMMUNICATIONS REVIEW OF A COMPANION MS.

ABSTRACT (246 words, 1,457 characters including spaces)

We measured the oxidation rates of N supplied as urea (UO) and ammonium (AO) in continental shelf and slope waters of the Southern Ocean west of the Antarctic Peninsula during the austral summer of 2018. The response of rates to substrate concentration varied by water mass. Rates increased moderately (up to 200%) with 440 vs 6 nM substrate amendments to samples from the Winter Water (WW, sampled at 35-100 m), but decreased (down to 7%) in samples from the Circumpolar Deep Water (CDW, 175-1000 m). AO rates decreased more than UO rates. This response suggests that CDW Thaumarchaeota are not well adapted to short-term variation in substrate concentrations and that even low amendments (we used 44 or 47 nM) may inhibit oxidation. Rates of AO and UO were not correlated; nor were they correlated with the abundance, or ratios of abundance, of marker genes; or with [NH₄⁺]; or [urea]. UO and AO were distributed uniformly across the study area within a water mass; however, they displayed strong vertical gradients. Rates in most samples from Antarctic Surface Water (ASW, 10-15 m) were below the limit of detection. Highest rates of both processes were in samples from the WW (21.2) and 1.6 nmol L⁻¹ d⁻¹ for AO vs UO, respectively) and CDW (7.9 and 2.5 nmol L⁻¹ d⁻¹), comparable to rates from the study area reported previously. The contribution of UO to nitrite production was ~24% of that from AO alone, comparable to ratios measured at lower latitudes.

INTRODUCTION (Main Text: 6,844 words; 42,059 characters including spaces.

Thaumarchaeota play an important role in the nitrogen cycle by oxidizing ammonia to nitrite (3-5), and they are abundant in Antarctic coastal waters (6-8). Identification of genes for putative ureases and urea transporters in Thaumarchaeota genomes (9, 10) suggested that these Ammonia-Oxidizing Archaea (AOA) might also be able to oxidize N supplied as urea. Subsequent work (11-13) demonstrated that the ability to oxidize urea-N is not universal in Thaumarchaeota, even among closely related isolates from the same environment. Alonso-Sáez et al. (14) used ratios of the abundance of Thaumarchaeota *ureC* to 16S rRNA (*rrs* hereinafter) or *amoA* genes, and incorporation into biomass of C supplied as urea, to infer that urea might be particularly important as a source of reduced N to Thaumarchaeota populations in polar (Arctic and Antarctic) waters. Results of their initial survey were replicated in subsequent work in the Arctic (15). Relatively few studies, and neither of these, have used ¹⁵N tracers to compare the oxidation rates of N supplied as urea (UO) and NH₄⁺ (AO) directly in the same sample. Recent work using ¹⁵N-labeled substrates (16-19) has demonstrated that the contribution of urea to nitrification in the open ocean can be significant, if highly variable.

There are few measurements of UO in samples from Antarctic waters, thus the contribution of urea-N to nitrite production there, relative to AO or other processes, is understudied and poorly constrained. A pilot experiment (20) found that the mean ratio of UO/AO in 3 samples from the Winter Water was 1.9, while it was 0.3 in 3 samples from the Circumpolar Deep Water. A 2018 cruise to continental shelf and slope west of the Antarctic Peninsula provided an opportunity to perform process studies and to compare the relative contributions of urea-N and NH₄⁺ to nitrite production in Antarctic coastal waters in a more robust data set. We examined the response of AO and UO to a range of substrate amendments to

gain insight into the factors controlling rates in situ and to evaluate the effect of tracer additions on measured rates. We assessed the effect of incubation temperature on rates to evaluate the significance to rate measurements of deviations of incubation temperatures from in situ, to determine if AOA from the study area were adapted to cold water, for comparison with the response of heterotrophs from the study area to water temperature, and to assess the potential response of polar nitrification to global warming. We examined the correspondence between AO and UO rates and genetic markers for these processes to evaluate the use of gene ratios (e.g. ref 14), as proxies for activity. Finally, we compared the relative contributions of UO and AO to nitrite production in Antarctic samples with other locations.

RESULTS AND DISCUSSION

Description of the study area. LMG1801 spanned 4 weeks during the Antarctic summer (6 January to 4 February, Supplemental Table 1) and sampled a strip of the continental shelf and slope west of the Antarctic Peninsula (WAP: Supplemental Figure 1) 700 km parallel to the coast (NE-SW) by 200 km perpendicular to the coast (NW to SE). This is a physically dynamic coastal ocean (21) in a region of extreme seasonality. There are 4 water masses in the study area (21, 22): Antarctic Surface Water (ASW, sampled at 10 or 15 m); the Winter Water (WW, sampled at the water column temperature minimum, 35-100 m depending on location); the Circumpolar Deep Water (CDW, sampled at 175–1000 m); and Slope water (SLOPE, samples from 2500 to 3048 m depth, generally ~10 m above the bottom at stations on the slope or over basins on the shelf). Our samples were collected from stations on the PAL LTER sampling grid (Supplemental Figure 1), though we only sampled 3 or 4 depths per station.

Response of AO and UO to ¹⁵N amendments. Environmental concentrations of NH₄⁺ and urea may fluctuate depending on localized coupling between regeneration and uptake or oxidation, subjecting nitrifiers to short-term temporal variation in substrate concentrations (e.g. 16, 23, 24). Further, detection of N oxidation rates may require amendments of ¹⁵Nlabeled substrates that significantly increase the concentration of total (labeled plus unlabeled) substrate in samples. Elevated substrate concentration may influence oxidation rates via enzyme kinetics (25) or metabolite inhibition (26). We performed experiments to evaluate the effect of tracer additions and variable

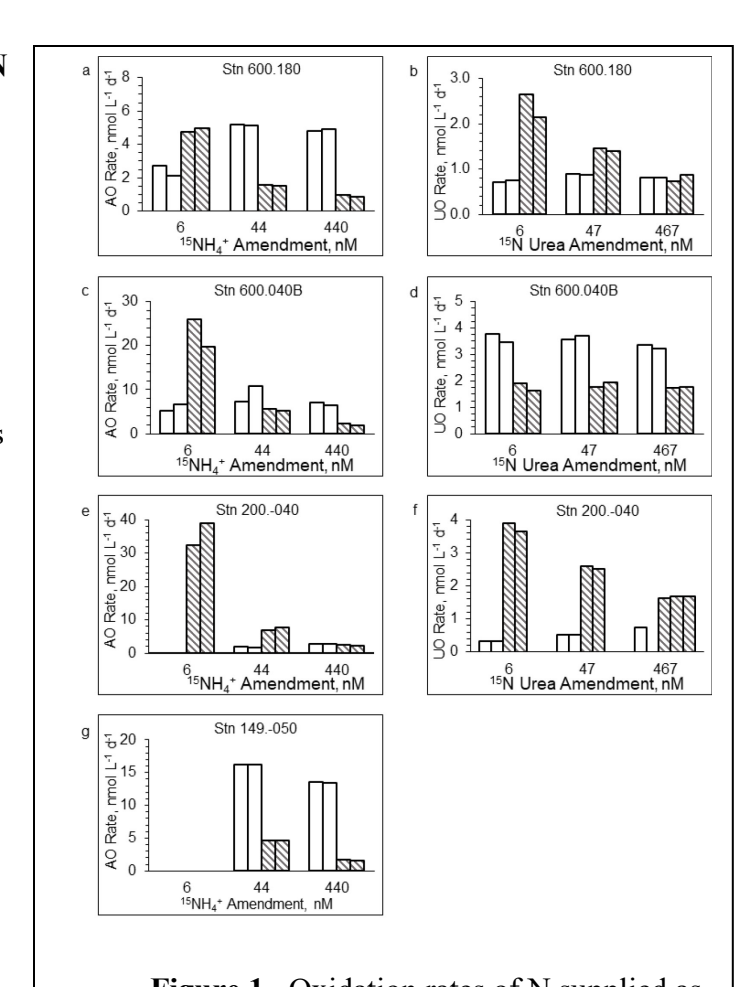


Figure 1. Oxidation rates of N supplied as NH₄⁺ (AO) or urea (UO) as functions of ¹⁵N-labeled substrate amendments (as nmol L⁻¹ of the substrate, not of N in the case of urea). Open bars are WW samples (70-80 m), cross-hatched bars are CDW samples (400-600 m).

substrate concentrations on nitrite production rates by AO and UO.

We found marked differences in the responses of WW versus CDW populations to ¹⁵N amendments. AO rates in WW samples increased with increasing amendments of ¹⁵NH₄⁺ (AO rate with a 440 nM amendment averaged 160% of the rate with a 6 nM amendment; Figure 1,

Table 1), while AO rates were reduced by increasing $^{15}NH_4^+$ amendments to CDW samples (rate with a 440 nM amendment averaged 12% of the rate with 6 nM; Figure 1, Table 1). This difference in response was significant (2-tail *t*-test p=0.022). A similar pattern emerged if AO rates with 44 nM amendments were compared to rates with 6 nM amendments (Figure 1, Table 1).

UO rates in WW samples also increased with increasing ¹⁵N-urea amendments (rates with 470 nM amendments averaged 105% of rates with 6 nM amendments, Figure 1, Table 1), while UO rates in CDW samples decreased with increasing urea amendment (rates with 470 nM amendments averaged 59% of the rates with 6 nM amendments). The same decrease was seen with 47 nM vs 6 nM amendments (Figure 1,

Table 1). The difference in response of UO rates to urea amendments in WW vs CDW samples was not significant (2-tail t-test p=0.15). CDW populations had a stronger response to NH₄⁺ than to urea amendments; however, the differences in the responses of WW or CDW populations to NH₄⁺ vs urea amendments were not significant.

Inhibition of AO and UO rates in response to elevated substrate concentrations has been observed previously, but the significance of the phenomenon has escaped attention. AO and UO rates measured in samples from the 1% light level (51 m) during a period of active upwelling (March 2015) at the SPOT station off southern California decreased in response to elevated (250 vs 15 nM) amendments to samples with ambient NH₄⁺ and urea-N concentrations of 10 and 190 nM (Figure 5 in ref (17). Although not discussed in their paper, Shiozaki et al. (19) found that urea amendments of 1,560 nM inhibited UO rates 50 to 77% relative to rates measured with 31 nM amendments (ambient [urea] 84-110 nM) in 3 samples from the 0.1% light level in the Beaufort Sea (calculated from their Supplemental Dataset 1). They did not test the effect of NH₄⁺

amendments on AO rates on this cruise; however, they performed similar experiments with ¹⁵NH₄⁺ amendments ranging from 31 to 1,560 nM using samples from the 0.1% light level at stations on a meridional transect of the North Pacific (24). These experiments (reported in their Figure 4a and Supplemental Table 1) showed no clear response of AO to amendments: AO rates increased in 6 and decreased in 7 samples where AO rates were greater than the limit of detection (>LD hereinafter). The mean change of AO rates with amendments of 1,560 nM versus 31 nM was 105% (range of 44-273%). The 31 nM ¹⁵NH₄⁺ amendments used in this study represent larger enrichments (194% to infinity, since ambient [NH₄⁺] was undetectable in some samples) than the 6 nM amendments to the samples used in our experiments (range 100-140% for both substrates).

A mechanism that might explain the response of CDW AOA to substrate amendments is sensitivity to reactive oxygen (ROS) and nitrogen (RNS) species. AOA are known to be inhibited by ROS and RNS species produced as a consequence of their metabolism (26-28) and previous work in our study area (27) verifies that these AOA populations are no exception. We hypothesize that ROS/RNS produced during the incubation can reach toxic levels in response to elevated substrate concentrations, including the 31 nM additions used as the lowest amendment by Shiozaki et al. (24), inhibiting further oxidation of N supplied as NH₄⁺ or urea. This response is similar to the response of AOA cultures to elevated [NH₄⁺] reported in Figure 3B of Kim et al. (26). Substrate concentrations, especially NH₄⁺, were generally lower in our CDW samples than in WW samples, thus the same ¹⁵NH₄⁺ or ¹⁵N-urea amendment represents a greater increase in substrate concentration in CDW than in WW samples (means over all samples, CDW vs WW: 700% vs 160% for NH₄⁺, 1,300% vs 1,000% for urea, Supplemental Table 2). The greater inhibition of CDW populations by NH₄⁺ vs urea may be due to the slower rate at which N from

Table 1. Response of nitrifiers to substrate amendments, summary of data from Figure 1. Concentrations of NH_4^+ or urea and the increase in total substrate concentration due to amendments, as a %, ((amendment + in situ)/in situ) x 100) are calculated for the samples used in the experiments, water mass means are reported. The ratio of the rates at higher amendments relative to rates measured at 6 nM are calculated from the means of duplicate rate measurements for each amendment, water mass means are reported. WW samples are from 70-80 m, CDW samples are from 400-600 m.

		Increase in substrate							
		concentration, % of			Rates with amendments			Ratio of Rates:	
	Substrate Concentration in situ, nM	unamended			of:			High/Low (%)	
									440 or
								44 or	470
				450 or			440 or	47 nM	nM
			44 or	467		44 or	470	versus	versus
	Substra	6 nM	47 nM	nM	6 nM	47 nM	nM	6 nM	6 nM
WW,	U 1								
¹⁵ NH ₄ ⁺	904	101	106	160	4.2	7.4	3.7	180	160
WW,									
¹⁵ N-Urea	52	112	200	1,000	1.6	1.7	1.5	130	105
CDW,									
¹⁵ NH ₄ ⁺	88	108	160	700	21.1	4.0	1.4	25	12
CDW,									
¹⁵ N-Urea	38	122	270	1,800	2.6	1.9	1.4	77	59

urea versus NH₄⁺ is oxidized, and thus ROS/RNS is produced, in these samples (21.2 vs 1.6 nmol L⁻¹ d⁻¹ for AO vs UO, respectively, in WW samples; 7.9 vs 2.5, with an outlier excluded, in CDW samples, Figure 1, Supplemental Table 2).

It is likely that sensitivity to, or production of, ROS/RNS varies among AOA clades (26). Gene ratios from samples collected on LMG1801 (Supplemental Figure 2), as well as more rigorous analyses performed previously (29-31), demonstrate that WW and CDW Thaumarchaeota populations are phylogenetically distinct. This difference may influence the rates at which they produce, or detoxify, ROS/RNS. Detoxification of ROS and RNS, regardless of its source, is also likely a community-level process (32, 33). Thus, differences in the composition of bacterioplankton communities in these two water masses may also play a role in the response of AOA to elevated substrate concentrations. Bacterioplankton and Thaumarchaeota populations in the winter mixed layer that becomes the Winter Water following water column stratification during spring (21, 22) may have been exposed to elevated concentrations of ROS generated by photochemistry, including photosynthesis. The concentration of one ROS compound, HOOH, has been shown to be higher in the surface mixed layer in the study area than at greater depths (27, 34). In contrast, the CDW water mass is always below the photic zone, thus CDW bacterioplankton and Thaumarchaeota populations would not have been exposed to photochemically produced ROS. These differences in exposure histories may exert selective pressure for ROS/RNS-tolerant bacterioplankton and Thaumarchaeota ecotypes in the WW relative to the CDW.

Our observations and those of others cited above suggest that amendments that increase substrate concentrations can significantly affect the rates measured, and not as expected from enzyme kinetic considerations. Over our entire data set, amendments of 44 nM ¹⁵NH₄⁺ increased

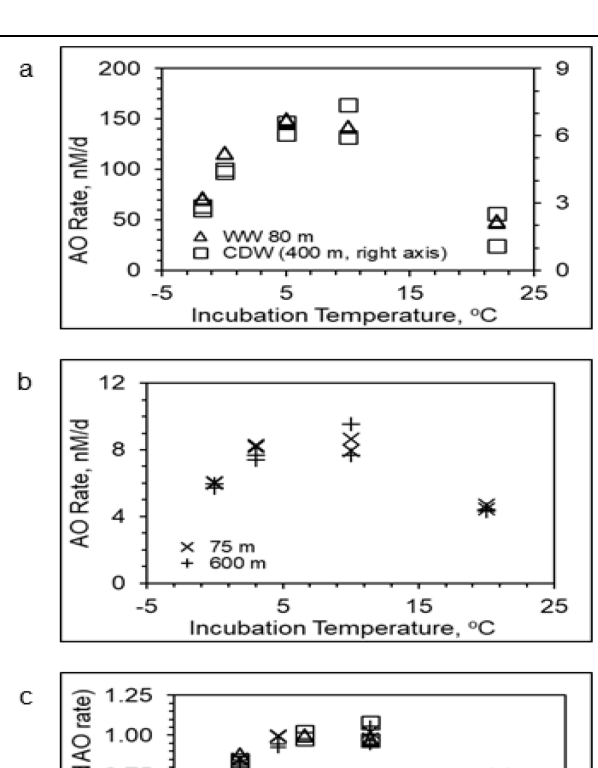
substrate concentrations 110±11% (mean ±SD) in WW samples and 150±28% in CDW samples.

15N-urea amendments (47 nM) increased WW concentrations by 310±370% and CDW concentrations by 290±190% (Supplemental Table 2). Assuming that AOA populations in all of our samples responded to substrate amendments similarly to amendments, the AO and UO rates we measured in WW samples overestimate the in situ rates by 180% and 130%, on average, while the AO and UO rates we measured in CDW samples are 25% and 77% of the in situ rates, on average (Table 1). We have not corrected the data reported in Supplemental Table 1 for these differences.

Rate measurements made in open ocean samples where [NH₄⁺] and [urea] are in the low nM range typically use substrate amendments that range from 30 to 50 nM, following recommendations from (25). Reported rates are thus likely to have been affected by the change in substrate concentration due to the tracer amendment. The problem isn't simply the kinetic effect of higher substrate concentrations on rates, but is likely a complex interaction between that and metabolite inhibition via the release of ROS/RNS. The data suggest that the effect is very nonlinear (Figure 2 in ref 17; figure 5 in ref 19; ref 26) and comparisons between rates measured with 30-50 nM additions and rates measured with much higher substrate additions may show little change because the threshold for inhibition is lower than 30-50 nM, (Figure 2, compare rates measured with 44 or 47 nM amendments with those measured with 440 or 470 amendments; Figure 4a in ref 19). Finally, our data suggest that, compared to WW populations, CDW Thaumarchaeota are poorly adapted to short term fluctuations in substrate concentrations that might arise from uncoupling (e.g. 16, 23, 24) or patchiness (35, 36).

Response of AO to incubation temperature. Production of $^{15}NO_x$ from $^{15}NH_4^+$ (we did not test urea) increased with temperature to maxima at 5-10 °C, then declined. The same pattern

was seen at two different stations and with both WW and CDW samples (Figure 2). Baer et al. (37) saw little change in nitrification rate with incubation temperature in samples from the Chukchi Sea (their figure 2), unlike the response of L-leucine incorporation (their figure 3). Their experiments were performed with samples taken from depths of 1–6.5 m and temperatures of -1.9–4.7 °C, while our experiments were performed with samples taken from WW and CDW water masses with mean environmental temperatures of -1.04 and 1.33 °C, respectively, (Supplemental Table 2) that do not vary greatly over a seasonal cycle. We found that rates were >LD in incubations at 0 °C at all stations and depths tested and were >LD in incubations at -1.0 °C in 3 of the 4 samples tested. This response suggests, not surprisingly, that the dominant ammonia oxidizers in shelf waters west of the Antarctic Peninsula are psychrophiles.



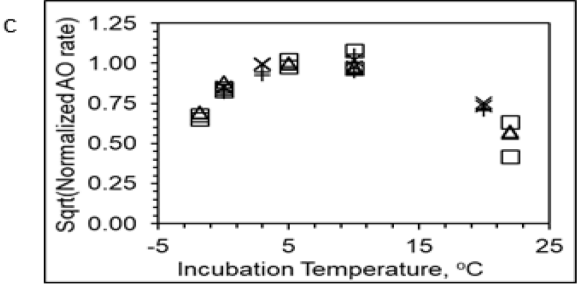


Figure 2. Response of AO rates to incubation temperature. Points from duplicate rate measurements overlap in some cases. Primary data (panel a, Station 168.-030; panel b, Station 600.040B) were transformed as the square root of the datum normalized against the highest rate recorded (panel c; (1, 2)).

The response of AO to incubation temperature contrasts with the response of heterotrophic activity in bacterioplankton populations in the study area sampled during a previous deployment (38). Heterotrophic activity, measured as ³H-labeled thymidine (TdR) or L-leucine (L-leu) incorporation, increased with incubation temperature over the range -1.4 to 10 ^oC (Supplemental Figure 4). We also compared our AO data to data from a more recent study of temperature adaptation in Antarctic bacterioplankton by Van Gestel et al. (2). We transformed our data as they did, as the square root of rates that were first normalized to the maximum rate in a sample (1, 39). This transformation linearized TdR and L-leu incorporation rate data (Supplemental Figure 3), but failed to linearize our AO rate data (Figure 2).

In contrast to the response to substrate amendments, the normalized data demonstrate that the response of AO rate to incubation temperature was the same for all of our samples, regardless of the water mass from which they were taken (Figure 2). This is consistent with heterotrophic activity measured in Bedford Basin, NS over a seasonal cycle by Li and Dickey (39). The T_{min} values of AO estimated using data from the two lowest incubation temperatures (Figure 2, Supplemental Table 3) were lower than those reported in Li and Dickey (39) or Van Gestel et al. (2), but in the range reported by Ratkowsky et al. (1) for cultures of psychrophilic heterotrophs. A potential explanation for the differences in response to elevated temperature between heterotrophs and ammonia oxidizers is that AO rates essentially measure the response to temperature of one reaction pathway in a guild of relatively low phylogenetic diversity, while heterotrophic activity as assessed by TdR or L-leu incorporation integrates the net result of cellular metabolism across many reaction pathways and over a phylogenetically diverse assemblage of microorganisms.

Mean Q₁₀ values for AO calculated for the interval 0 to 3 or 5 °C averaged 2.24 (Figure 2, Supplemental Table 3), similar to the value (1.1) reported by (37). The Percival® incubator we used maintained sample temperatures at (median, max, min) 0.25, 2.85, -1.50 °C, while *in situ* temperatures for our samples were: WW, -1.16, 0.16, -1.69; and CDW, 1.40, 2.04, -0.78. The medians of AO rates measured in WW and CDW samples are 9.0 and 5.1 nmol L⁻¹ d⁻¹. Assuming Q₁₀=2.24 applies to all of our samples, medians of AO rates in situ would be 8.0 and 5.6 nmol L⁻¹ d⁻¹, or 0.89 and 1.1 times the rates we report. We assume this correction would apply to UO rates as well. We have not been corrected the data reported in Supplemental Table 1 for the ~10% error due to differences between in situ and incubation temperatures.

Variation within water masses. The WAP has a strong seasonal cycle and complex physical oceanography tied, in part, to melting ice. We examined data from the WW and CDW water masses to determine if they displayed a temporal signal by splitting the data set into two groups representing samples collected at the beginning (days 1-15, n=104) versus end (days 16-29, n= 60) of the cruise. We used Mann-Whitney ranks tests of the null hypothesis that variables were distributed uniformly between these two groups (Supplemental Table 4). UO rate was the only variable with a significant (p<0.05) temporal signal. UO rates were higher (8.4 vs 1.2 nmol L⁻¹ d⁻¹) in CDW samples collected near the beginning of the cruise.

We used the same approach to determine if there were gradients in the distributions of variables within a water mass across the study area (Supplemental Figure 4). We restricted our analysis to WW and CDW water masses as many of the values for some variables were <LD in samples from the ASW and SLOPE water masses. We grouped samples by station location (northeast, n=88 versus southwest, n=76; and inshore, n=86 versus offshore, n=78), as shown in Supplemental Figure 1. AO rate was higher in CDW samples from the NE end of the sampling

grid (10.4 vs 3.2 nmol L⁻¹ d⁻¹, p<0.05) and at inshore stations (9.0 vs 4.9 nmol L⁻¹ d⁻¹, p<0.05). UO rates were greater in WW and CDW samples from stations on the NE end of the sampling grid (2.0 vs 0.8 nmol L⁻¹ d⁻¹ and 8.8 vs 1.4 nmol L⁻¹ d⁻¹, respectively; p<0.05; Supplemental Table 4). WW samples were both warmer and saltier at the NE end of the sampling grid, while the CDW was warmer at offshore stations (Supplemental Table 4).

Differences between water masses. Ammonium concentrations were greatest in samples from the ASW and WW, with mean concentrations of 930 and 640 nM that were not significantly different (Supplemental Table 2, Supplemental Table 5). Ammonium concentration decreased with depth to mean concentrations of 160 and 200 nM in CDW and SLOPE samples, respectively. Urea concentrations were generally lower than those of NH₄⁺ (averages of 130 versus 510 nM over all samples), with no statistically significant differences among water masses (Supplemental Table 2, Supplemental Table 5). Both data sets contained outliers that were excluded from these calculations and NH₄⁺ data are missing for some samples. The mean ratios of N available as urea versus NH₄⁺ were 0.35, 0.32, 0.95 and 0.31 in ASW, WW, CDW and SLOPE water samples, respectively, if one outlier from a SLOPE water sample (urea concentration 1,800 nM, resulting in a urea-N/NH₄⁺ ratio of 57) is excluded.

We evaluated the distribution of selected genes of significance to nitrification in 31 to 93 different samples (Supplemental Table 1, Supplemental Figure 2). The abundances of all of the genes we measured were statistically significantly different between the 4 water masses we sampled (Supplemental Table 5).

The mean abundance of 16S rRNA (rrs hereinafter) from Bacteria decreased with increasing depth from 1.3 x 10 9 copies L⁻¹ in ASW versus 0.012 x 10 9 copies L⁻¹ in SLOPE water. In contrast, the mean abundance of Thaumarchaeota rrs increased from 0.6 x 10 6 copies

 L^{-1} in samples from ASW to ~10 x 10^6 copies L^{-1} in WW and CDW samples, then decreased to 2.4×10^6 copies L^{-1} in SLOPE water samples. As a consequence of these distributions, the contribution of Thaumarchaeota to prokaryotes increased with depth, from a mean of 0.2% in ASW samples to a mean of 26% in SLOPE water samples.

We measured the abundances of Thaumarchaeota amoA genes on LMG1801 using the Mosier and Francis (40) WCA and WCB primer sets. Mean concentrations (WCA+WCB) were 0.26 and 4.0 x 10⁶ copies L⁻¹ in WW and CDW samples, respectively (Supplemental Table 2). These values are significantly lower than concentrations determined previously (LMG1101, ref 31) in samples from the same water masses using the Wuchter et al. (41) primer set (4.1 and 12.5 x 10^6 copies L⁻¹, p < 0.0001 and p = 0.0002, respectively). We also found that the ratios of amoA/rrs genes in a given sample (Supplemental Figure 2a) were lower on LMG1801 than LMG1101: 0.02 versus 1.7 (p < 0.0001) and 0.46 versus 1.6 (p = 0.0005) for WW and CDW, respectively. The same rrs primers (42) were used in both studies, yielding 10 versus 2.9 and 10 versus 16 x 10⁶ cells L⁻¹ for WW and CDW samples collected on LMG1801 versus LMG1101. While some of the difference in *amoA* abundance estimates may be attributed to interannual variability in the actual abundance or composition of Thaumarchaeota at the study site, it is more likely that the discrepancy resulted from primer bias. Most of the amoA genes we detected in samples from LMG1801 were amplified by the WCB (deep water) primer set, regardless of depth: mean 72-100% with an average of 96% over all samples. Phylogenetic analysis (31) suggested that most of the Thaumarchaeota amoA genes in our samples should be amplified by the WCA (shallow water) primer set.

We quantified the distribution of *rrs* from *Nitrospina*, a dominant clade of nitrite oxidizers in the sea, because of their potential to contribute to urease activity (43-45). *Nitrospina*

rrs (46) was detected throughout the water column (Supplemental Table 1) with greatest mean abundances in the WW and CDW water masses (0.7 and 0.6 x 10^6 copies L⁻¹, respectively, which were not significantly different: p = 0.095, Supplemental Tables 2 and 5). The abundances of *Nitrospina rrs* in ASW and SLOPE water masses were lower and they were not significantly different from each other (mean abundances of 0.09 versus 0.18 x 10^6 copies L⁻¹, respectively, p = 0.50, Supplemental Tables 2 and 5).

Thaumarchaeota ureC genes (14) were also distributed throughout the water column, with greatest mean abundance (1.2 x 10^6 copies L⁻¹, Supplemental Table 2) in the CDW water mass. The distribution of Thaumarchaeota ureC was similar to that of Thaumarchaeota rrs and $Nitrospina\ rrs$, with lower concentrations in the ASW and SLOPE water masses (0.032 and 0.050 x 10^6 copies L⁻¹, respectively, not significantly different, Supplemental Tables 2 and 5). Mean ratios of Thaumarchaeota ureC/rrs were 0.15 for samples from the ASW, 0.17 for the WW (mean 0.05 if an outlier is set aside), 0.13 for the CDW, 0.02 for the SLOPE and 0.14 over all depths (mean 0.09 if the WW outlier is set aside). Kruskal-Wallis ranks tests demonstrated that the ratios differed by water mass (Supplemental Table 5). Mann-Whitney ranks tests revealed that the median ratio for CDW samples was significantly (p<0.0001) greater than ratios for WW and SLOPE data, but that median ratios for the other pairwise comparisons were not significantly different (p>0.01).

 15 N oxidation rates were <LD (<4.3 and <0.6 nmol L $^{-1}$ d $^{-1}$ for AO and UO, respectively) in many of the samples we collected (Supplemental Table 2). Means over all samples (values <LD set to 0, ref 47) of the oxidation rates of N supplied as NH₄ $^+$ or urea were 10.9 (n=214, range 0-158) and 2.6 (n=215, range 0-120) nmol L $^{-1}$ d $^{-1}$, respectively (Supplemental Table 2). The highest UO rates (114 and 120 nmol L $^{-1}$ d $^{-1}$) were from replicates of one CDW sample with

an elevated urea concentration (2,060 nM). If these outliers are removed, the mean rate of UO is 1.5 nmol L⁻¹ d⁻¹ (range 0-14).

Rates of AO and UO differed significantly between water masses (p=0.008, Supplemental Table 5). The AO and UO rates measured in most of the samples collected from the ASW and SLOPE water masses were <LD (Supplemental Table 1). Rates measured in the WW averaged 21 and 1.6 nmol L⁻¹ d⁻¹, while those in samples from the CDW averaged 7.9 and 2.5 (outliers excluded) nmol L⁻¹ d⁻¹ for AO and UO, respectively (Supplemental Table 2).

Relationships among variables. We found statistically significant correlations between the abundance of *Nitrospina rrs* genes and AO or UO rates (Supplemental Figures 5 and 6, Supplemental Table 6; AO all data: R^2 =0.43, p=0.001; UO all data: R^2 =0.21, p=0.004). The relationships were stronger for WW samples than for CDW samples (Supplemental Table 6). The "reciprocal feeding" model (48) for the role of *Nitrospina* in ammonia oxidation predicts a positive relationship between *Nitrospina* abundance and AO. While urease activity associated with *Nitrospina* may be an explanation for the correlations we observed, the correlation could also be based on other factors, such as urea supply or the rate of nitrite production in a sample by combined AO + UO.

The abundance of *ureC* genes was significantly correlated with the abundance of Thaumarchaeota *rrs* and *amoA* genes (Supplemental Table 6). We found no significant correlations between the abundance of *ureC* genes and either [NH₄⁺] or [urea], or with the ratio ([urea-N]/[NH₄⁺]), or with an index of the contribution of urea-N to oxidizable N ([urea-N]/([urea-N] + [NH₄⁺]) in any of the water masses we sampled (Supplemental Figure 2, panels g and h). This index does not account for the potential contribution of other sources of oxidizable N, such as cyanate (45), that we did not measure. The ratio of Thaumarchaeota *ureC* to

Thaumarchaeota rrs genes was greatest in CDW samples (regression slope = 0.13, mean of the ratio of ureC/rrs for data from the same sample = 0.13) and distinct from the ratio in WW samples (regression slope 0.03, mean ratio of ureC/rrs = 0.05; Supplemental Figure 2, Supplemental Table 2).

These ureC/rrs ratios are lower than those reported by Alonso-Sáez et al. (14): 0.09 vs 0.76 for all of their data, 0.09 vs 0.51 with an outlier removed, (p<0.0001 in both cases); and did not increase with depth (model 2 r = -0.13, p=0.08). We examined their data, reported in their supplemental tables S4 and S5. We found that the relationship between Thaumarchaeota ureC/rrs and depth was strongly influenced by the value of one outlier that was based on a ureC analysis with a very high standard deviation (mean \pm SD = 21.95 \pm 10.09). The correlation between the ratio of Thaumarchaeota ureC/rrs and depth was not statistically significant, regardless of whether the outlier is included (R^2 =0.030, p=0.15), or not R^2 =0.034, p=0.16). Within the CDW data set that was the basis for the conclusion that Thaumarchaeota ureC/rrs ratios increase with depth, the mean Thaumarchaeota ureC/rrs ratio was 2.67, but without the outlier it was 1.04. We conclude that the ratio of the abundance of Thaumarchaeota ureC/rrs is not a good predictor of the contribution of urea to nitrification, and that there seems to be little change with depth in the contribution of urea to nitrification, at least in the WAP.

We compared the distribution of AO and UO to the distribution of relevant marker genes and environmental variables (Supplemental Figures 5 and 6, Supplemental Table 6). Rates that were <LD were set to 0 for this analysis, although using all data yielded essentially the same result. AO rates correlated weakly with the abundances of Thaumarchaeota and *Nitrospina rrs* genes (Supplementary Figure 5, Supplemental Table 6: for all samples, Thaumarchaeota *rrs* genes r=0.26, p=0.002; *Nitrospina rrs* genes r=0.48, p=0.001). UO rates correlated significantly

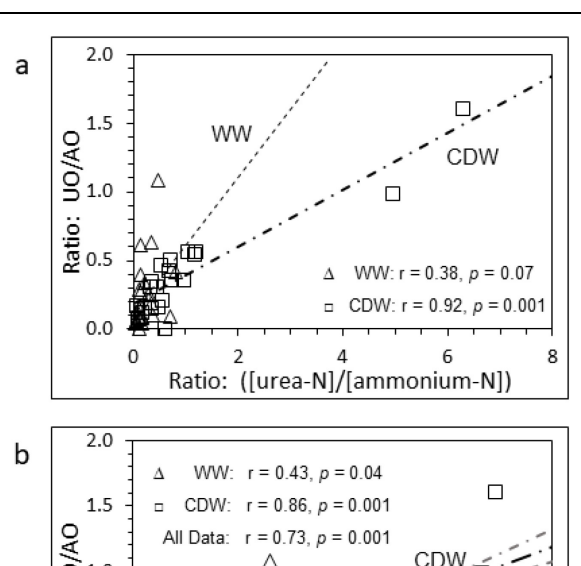
with abundances of *Nitrospina rrs* genes when all samples were considered together (Supplemental Figure 6, Supplemental Table 6). Significant correlations between UO rates and gene abundances were also obtained when data from WW and CDW water masses were analyzed separately, though slopes of relationships for CDW samples were negative (WW: r=0.39, 0.44, 0.49 and 0.41 and CDW: r=-0.31, -0.26, -0.27 and -0.18 for UO rate versus Thaumarchaeota *rrs*, *amoA*, *ureC* and *Nitrospina rrs*, respectively, Supplemental Table 6). AO rates were significantly positively correlated with [NH₄⁺] in CDW samples (Supplemental Figure 5, Supplemental Table 6). UO rates were significantly positively correlated with both [NH₄⁺] and [urea] in CDW samples.

We compared the means for each sample of duplicate measurements of AO and UO, where both rates were >LD. The two rates were not correlated: r=0.12, p=0.24 for WW samples and r=0.13, p=0.14 for CDW samples (Figure 3). We also used mean rates to calculate the ratios of rates. The mean ratio of UO/AO from the complete data set (n=45) was 0.38 with a range of 0.02-6.6 (Supplemental Table 2). The ratio of 6.6 was from one sample with an unusually high urea concentration. The mean ratio is 0.24, with a range of 0.02-0.94, when this outlier is excluded from the calculation. Ratios of UO/AO measured in the WW water mass averaged 0.17 while those in samples from the CDW water mass averaged 0.69 (0.35 with the outlier excluded). These values are significantly different (Mann-Whitney ranks tests, p=0.013, CDW outlier removed). Wan et al (2021), also found that UO/AO increased with depth based on samples from 4 depths at 4 stations in the north Pacific.

Contribution of urea-N to nitrification. We explored the relationships between rates and variables, or combinations of variables, related to AO and UO to determine if they could be used to predict activity. We found no statistically significant relationships between UO and

[NH₄⁺] or [urea] when all samples were considered together, or in the subset of WW samples. We found that UO was positively correlated with [NH₄⁺] and [urea] in CDW samples (Supplemental Table 6), indicating that UO was not inhibited by [NH₄⁺], in contrast to results from experiments with Chukchi Sea populations (19).

UO correlated significantly with the contribution of urea-N to oxidizable N when all samples were considered together (p=0.003), but the correlation was weak (r=0.23) and was not significant when considered by water mass (Supplemental Table 6). The ratio of rates (UO/AO) was predicted by the ratio of [urea-N] to [NH₄⁺] (Figure 4, panel a); however, this relationship was not consistent between water masses (WW slope = 0.49, r=0.38, CDW slope = 0.21, r=0.92). The best predictor of UO/AO in a sample was the index of the contribution of urea-N to



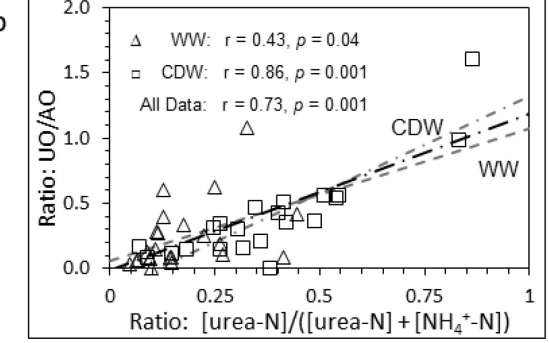


Figure 4. Ratio of the oxidation rates of urea-N to NH₄⁺-N (UO/AO) versus: a) the ratio of [urea-N] to [NH₄⁺-N] measured in the same sample; and b) the contribution of urea-N to oxidizable N ([urea-N]/([urea-N] + [NH₄⁺-N])). UO and AO are means of replicate rate measurements made for a particular sample (station and depth). Model 2 OLS regression lines, correlation coefficients and *p*-values for the correlation are shown. The heavy regression line in panel b) is for all data (WW + CDW combined).

oxidizable N in the same sample (Figure 4) panel b). With the caveat that the number of samples from each water mass with data allowing the calculation of both parameters was small, we found that the strength of this relationship differed between water masses: r=0.43 for WW samples, but r=0.86 for samples from the CDW and r=0.73 for the combined WW+CDW data set. The slopes of the regressions (Figure 4: 1.01, 1.48 and 1.19 for WW, CDW and All Data, respectively) were not significantly different (p<0.05). However, neither of these parameters was a good predictor of the absolute rate of UO. And, while we found a strong relationship between UO/AO and ([urea-N]/([urea-N]+[NH₄⁺])) in our data set, this relationship does not hold for data from studies of other locations (Gulf of Mexico, ref 18; Arctic

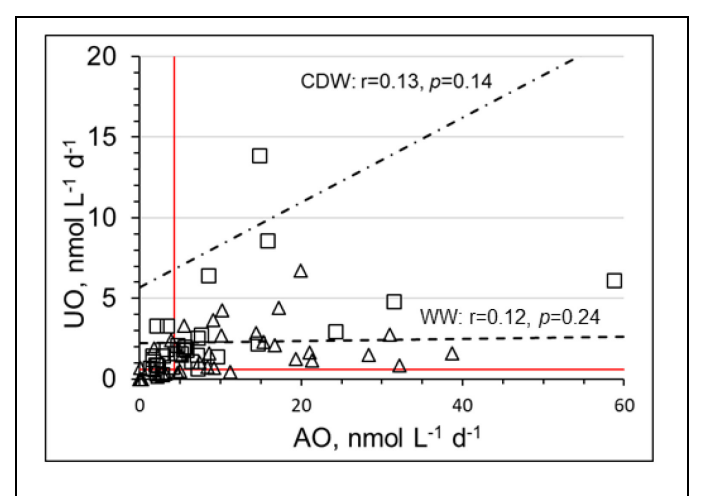


Figure 3. Oxidation rates of urea-N versus NH₄⁺-N. Data points are means of the UO and AO rates measured for a given sample. Red horizontal and vertical lines indicate the limits of detection estimated for these measurements. Model 2 ordinary least squares regressions are calculated from values greater than the limits of detection. Outliers (WW: 114, 2.5 and 101, 3.8; CDW: 17.8, 117) have been omitted from the plot but were included in the regressions. Samples from the WW are shown as Δ , samples from the CDW are shown as \Box , and samples of SLOPE water are shown as X.

Ocean, ref 19), where all variables required for this analysis are available.

Supplemental Table 7 compares data from LMG1801 with ratios of the oxidation rates of N supplied as urea versus NH₄⁺ (UO/AO) calculated from data in other studies. Values range from very small contributions of urea to nitrite production (Gulf of Mexico) to urea supplying most of the N oxidized to nitrite (WAP WW in 2011, deep water at the SPOT time series station, Bering/Chukchi Seas). Data from LMG1801 indicate that urea-N contributed significantly to nitrification on the continental shelf west of the Antarctic Peninsula, and that it was relatively more important as the contribution of urea to oxidizable N increases. We found no relationship between UO/AO and measures of the relative availability of urea N in the other data sets we examined, including our data from the SAB (20). The SPOT data set (17) suggests an increase with depth in the contribution of urea to nitrification, as do data presented in Wan et al. (16), and as we found on LMG1801; however, data reported in Shiozaki et al. (19) have the opposite trend (contribution of UO decreases with depth). These data demonstrate that the contribution of urea to nitrification in the open ocean can be significant, but it appears to be highly variable, and the data do not support the general conclusion that the contribution of urea N to nitrite production is enhanced in polar waters relative to sites at lower latitudes (14).

CONCLUSIONS

The response of N oxidation rates to elevated substrate concentrations was complex, with rates increasing slightly in WW samples, but strongly inhibited in CDW samples, and inhibition was greater for NH₄⁺ than urea amendments. We hypothesize that the inhibition at elevated substrate concentrations may have been caused by increased production of reactive oxygen or nitrogen species accompanying oxidation of NH₄⁺ or urea-N. This may be a general problem for rate measurements made in open ocean samples from below the photic zone and suggests that

deep water Thaumarchaeota populations are not well-adapted to short-term fluctuations in substrate concentration. Urea-N contributed significantly to the production of nitrite in samples from the continental shelf and slope west of the Antarctic Peninsula. Oxidation rates of urea-N were 24%, on average, of the oxidation rates of NH₄⁺, similar to the contribution of urea to nitrite production at lower latitudes. Oxidation rates of urea-N were not correlated with the ratio of Thaumarchaeota *ureC*/16S rRNA, nor with [NH₄⁺], [urea] or rates of NH₄⁺ oxidation. Oxidation of urea-N was not inhibited by elevated NH₄⁺ concentrations. Ammonia oxidation exhibited a psychrophilic response to manipulations of incubation temperature, which differed from heterotrophic activity.

MATERIALS AND METHODS

A more detailed description of sample collection, processing and analysis is presented in the Supplemental Material linked to this article.

Sample Collection. We sampled the continental shelf and slope west of the Antarctic Peninsula (Supplemental Figure 1) during the austral summer of 2018 (ARV Laurence M Gould cruise LMG1801, PAL-LTER cruise 26, DOI: 10.7284/907858). Sampling focused on 3 or 4 depths at each station, chosen to represent Antarctic Surface Water (ASW, samples from 10 or 15 m), Winter Water (WW, samples from 35 to 100 m, targeting the water column temperature minimum), Circumpolar Deep Water (CDW, samples from 175 to 1000 m depth) and slope water (SLOPE, samples from 2500 to 3048 m depth, generally ~10 m above the bottom at stations on the slope or over basins on the shelf). Water was collected in Niskin bottles (General Oceanics Inc., Miami, FL, USA). Samples for DNA and nutrient analyses were drained into

opaque 2 L HDPE plastic bottles. Water for incubations was drained into aged, acid-washed, sample-rinsed polycarbonate bottles.

DNA samples were filtered under pressure through 0.22 µm pore size Sterivex filters (EMD Millipore, Billerica, MA, USA). Residual seawater was expelled, then lysis buffer was added to the filter capsule, which was capped, frozen, then stored at -80 °C. Samples of the Sterivex filtrate were frozen at -80 °C for subsequent chemical analyses. One set of filtrate samples was stored briefly at 4 °C, then used for onboard determination of ammonium concentration by the *o*-phthaldialdehyde method (49).

Gene abundance. DNA was recovered from Sterivex filters using a lysozyme and proteinase K digestion, followed by purification by phenol-chloroform extraction. Archaea and Bacteria genes in the extracts were quantified by PCR (qPCR). The primers and probes used, PCR reaction conditions and our estimates of the precision of the measurements are given in Supplemental Table 8.

Nitrogen oxidation rates. AO and UO were measured using ¹⁵N-labeled substrates. Substrates were added to samples within ~1 hr of collection to yield ~44 nM of ¹⁵NH₄⁺ (25, 50, 51) or ~47 nM of urea (94 nM of urea ¹⁵N). These amendments increased substrate concentrations in the samples by an average of 26 and 190%, range: 2-120% and 2-1,800% for NH₄⁺ and urea, respectively. Labeled substrates were added to duplicate bottles that were incubated in the dark for ~48 hr. Incubation temperature averaged 0.23 °C with a standard deviation of 0.71 °C. Incubations were terminated by decanting ~40 mL subsamples into plastic tubes that were immediately frozen at -80 °C.

We ran experiments with samples from 2 depths at 3 stations (Supplemental Figure 7) to verify that ¹⁵N oxidation rates did not change significantly during incubations, to assess the

effect of substrate amendments on measured rates, and to assess the effect of incubation temperature on measured rates. Rates calculated from single-point determinations, (end-points of samples from the survey, from experiments, or the 48 hr points from time courses), agreed well with rates estimated from the slopes of regressions of time course data (Supplemental Table 9). Rates estimated from slopes were generally lower than rates calculated from end-point determinations, which assume intercepts of 0, while intercepts of regressions ranged from -0.25 to 1.41 nmol L⁻¹

¹⁵N in nitrite plus nitrate. The ¹⁵N content of NO₂⁻ plus NO₃⁻ (¹⁵NO_x) of our samples was measured using the 'denitrifier method' (52) with *Pseudomonas aureofaciens* as described previously (51). The N₂O produced was analyzed using a Gas Bench II coupled to a Finnegan MAT 252 mass spectrometer (53, 54), following the recommendations of Casciotti et al. (55).

Rate calculations. Our rate measurements are based on the production of $^{15}NO_x$ from ^{15}N labeled substrates. We calculated oxidation rates by comparing $\delta^{15}N$ values of the NO_x pool at the ends of the incubations with values in unamended samples ("natural abundance"), as described previously (51). We assumed that the $\delta^{15}N$ value of naturally occurring ammonium and urea is the same as that of AIR. Chemical data needed for rate calculations were not available for some samples (see Supplemental Table 1), so we substituted water mass averages (Supplemental Table 2) determined from other samples taken on the cruise. Samples with low or no activity sometimes yielded negative rates because the $\delta^{15}NO_x$ "natural abundance" value for that sample was greater than the $\delta^{15}NO_x$ value determined for the amended treatment sampled at the end of the incubation. Note that the rates we report are for N oxidized, regardless of whether it was supplied as NH_4^+ or urea.

Precision and accuracy. Analytical uncertainty of $\delta^{15}N$ measurements ranged from 0.36‰ to 0.56‰. Accuracy was 0.42‰ (at-% $^{15}N = 0.00019$, n = 56). The precision of nitrite+nitrate analyses run by LTER personnel was reported to be 100 nM. We determined the precision of ammonium and urea analyses as the mean standard deviation of replicate (2 or 3) analyses of a given sample. They are: ammonium, 65 nM; urea, 10 nM. We ran Monte Carlo simulations to estimate the precision of rate measurements, which are 2.2 nmol L⁻¹ d⁻¹ for AO and 0.31 nmol L⁻¹ d⁻¹ for UO, or relative standard deviations (RSD; ((standard deviation/mean) x 100)) of 15% and 11%, respectively, of calculated rates. The limit of detection for a measurement was set at 1.96 times the precision of the measurement.

Statistical analyses. Rates that were below the limits of detection as established above were assigned values of 0 (47). Outliers were defined as values >(3rd quartile + (1.5 * IQR)) where IQR = Intra Quartile Range. We tested for spatial gradients in the distributions of variables across the study area within a water mass (Supplemental Figure 4) by grouping stations by location (northeast versus southwest, inshore versus offshore), as shown in Supplemental Figure 1. Assignments of individual stations to these groups are given in Supplemental Table 1. We used Mann-Whitney ranks tests to determine if variables were distributed uniformly across the study area within a water mass, and Kruskal-Wallis ranks tests of significant differences between the 4 water masses sampled. Variables that were not uniformly distributed among water masses (most of them) were analyzed further using *post hoc* Dunn tests, with *p*-values adjusted for false discovery rate using the Benjamini-Hochberg correction, to identify sets that differed significantly at p<0.01. Pearson product moment regressions run in VassarStats (http://vassarstats.net/, $^{\circ}$ R. Lowry) were used to obtain slopes of time courses. We used model 2 ordinary least square regressions run in R (56) to test for correlations between variables.

Data archives. The data we collected on LMG1801 are archived by the Biological and Chemical Oceanography Data Management Office. The data used in the analyses presented here are from Supplemental Table 1, with summaries by water mass given in Supplemental Table 2.

CONFLICTS OF INTEREST (7 words, 45 characters including spaces)

The authors declare no conflicts of interest.

ACKNOWLEDGMENTS (121 words, 733 characters including spaces)

We thank the officers and crew of the ARSV Laurence M Gould and staff of Raytheon Polar Services Company, especially Diane Hutt, for their support during cruise LMG1801, and personnel affiliated with the Palmer LTER (funded through Grant NSF PLR 1440435) for additional support on LMG1801 and for subsequent access to project data. We would also like to thank S. Rauch at BCO-DMO for her assistance in archiving the data from this project. JTH would like to thank reviewers for constructive comments that helped improve the MS, and T. Hastings for just being there. This work was supported by the US National Science Foundation through grants OPP 1643466, (to JTH) and OPP 1643354 (to BNP). This is SOEST contribution number XXXX.

AUTHOR CONTRIBUTIONS (40 words, 227 characters including spaces)

JTH and BNP designed the research; JTH, BNP and HD conducted the sampling program; JTH, JD, AO-O, NJW, TA and BNP contributed to sample analysis; JTH and BNP analyzed the data, JTH wrote the paper with input from the coauthors.

Figure 1. Oxidation rates of N supplied as NH₄⁺ (AO) or urea (UO) as functions of ¹⁵N-labeled substrate amendments (as nmol L⁻¹ of the substrate, not of N in the case of urea). Open bars are WW samples (70-80 m), cross-hatched bars are CDW samples (400-600 m).

Figure 2. Response of AO rates to incubation temperature. Points from duplicate rate measurements overlap in some cases. Primary data (panel a, Station 168.-030; panel b, Station 600.040B) were transformed as the square root of the data normalized against the highest rate recorded (panel c; (1, 2)).

Figure 3. Oxidation rates of urea-N versus NH_4^+ -N. Data points are means of the UO and AO rates measured for a given sample. Red horizontal and vertical lines indicate the limits of detection estimated for these measurements. Model 2 ordinary least squares regressions are for values greater than the limits of detection. Outliers (WW: 114, 2.5 and 101, 3.8; CDW: 17.8, 117) have been omitted from the plot but were included in the regressions. Samples from the WW are shown as Δ, samples from the CDW are shown as \Box , and samples of SLOPE water are shown as X.

Figure 4. Ratio of the oxidation rates of urea-N to NH₄⁺-N (UO/AO) versus: a) the ratio of [urea-N] to [NH₄⁺-N] measured in the same sample; and b) the contribution of urea-N to oxidizable N ([urea-N]/([urea-N] + [NH₄⁺-N])). UO and AO are means of replicate rate measurements made for a particular sample (station and depth). Model 2 OLS regression lines, correlation coefficients and p-values for the correlation are shown. The heavy regression line in panel b) is for all data (WW + CDW combined).

Table 1. Response of nitrifiers to substrate amendments, summary of data from Figure 1. Concentrations of NH₄⁺ or urea and the increase in total substrate concentration due to amendments, as a %, ((amendment + in situ)/in situ) x 100) are calculated for the samples used in the experiments, water mass means are reported. The ratio of the rates at higher amendments relative to rates measured at 6 nM are calculated from the means of duplicate rate measurements for each amendment, water mass means are reported. WW samples are from 70-80 m, CDW samples are from 400-600 m.

Supplemental Figure 1. Chart of the study area. The orange double line separates stations assigned to the NE vs SW groups. Symbols for nearshore stations are green squares, symbols for offshore stations are blue circles. Stations used to validate our experimental protocols are indicated by an x. Line numbers correspond to the PAL LTER (https://pallter.marine.rutgers.edu/) grid numbering system. Base map courtesy LTER Network Office (https://lternet.edu/).

Supplemental Figure 2. Biplots of gene abundances by water mass. ASW omitted because of minimal data. a) Thaumarchaeota amoA vs Thaumarchaeota rrs, b) Thaumarchaeota ureC vs Thaumarchaeota amoA, d) Thaumarchaeota ureC vs Nitrospina rrs, e) Thaumarchaeota ureC vs [urea], f) Thaumarchaeota ureC vs [NH4+], g) Thaumarchaeota ureC vs ([urea]/[NH4+]), h) Thaumarchaeota ureC vs [urea-N]/([urea-N]+[NH4+]). Slopes, coefficients of determination and p-values of the correlation ("NS" = p>0.05) are from Model II ordinary least squares regressions. Trend lines are shown for significant (p<0.05) regressions. The legend in panel a) shows line styles used for each water mass. Samples from the WW water mass are shown as Δ , samples from CDW are

shown as □, and samples from SLOPE water are shown as X. Some points have been omitted from the plots (see panels) to improve the resolution of points near the origins. One CDW outlier was omitted from the plot and the regression shown in panel c).

Supplemental Figure 3. Effect of incubation temperature on heterotrophic activity in a sample of surface water collected near Spume Island. Unpublished data from (Hollibaugh et al. 1992). Rate data (panels a, b) were transformed as the square root of rates normalized against the rate at 10 °C (1, 2) in panels c and d.

Supplemental Figure 4. Distribution of variables related to the oxidation of NH₄⁺ or urea-N across the study area, by water mass. The data for a given variable from a given water mass were tested (see Supplemental Table 5) for random distribution between pairs of geographic groups as indicated in Supplemental Figure 1. See Supplemental Table 2 for assignments of individual stations to groups. The area of the circles on each of the plots is scaled to values of the variable, with a key given at position: (latitude, longitude) -62, -76 on each panel. The key also shows the locations of all samples taken from a given water mass. Measurements that were less than the limits of detection have been set to 0 and thus are not shown on the plots. Sample temperatures were re-scaled to values >0 °C by adding 2 °C to all measured values. Base map courtesy LTER Network Office (https://lternet.edu/). Columns (left to right): 1, abundance of Bacteria 16S rRNA genes (rrs, 10⁹ copies L⁻¹, LD=0.01); 2, Thaumarchaeota 16S rRNA genes (rrs, 10³ copies L⁻¹, LD=3.9); 3, Thaumarchaeota ammonia monooxygenase genes (amoA, 10^3 copies L⁻¹, LD=2.0); 4, the α subunit of Thaumarchaeota urease (ureC, 10³ copies L⁻¹, LD=15.7); 5, Nitrospina 16S rRNA genes (rrs, 10³ copies L⁻¹, LD=3.9); 6, oxidation rate of NH₄⁺ N (AO, nmol L⁻¹ d⁻¹, LD=4.3); 7, oxidation rate of urea-N (UO, nmol L⁻¹ d⁻¹, LD=0.61); 8, sample temperature (°C + 2); 9, sample salinity (PSU).

Supplemental Figure 5. Oxidation rates of N supplied as NH_4^+ (AO) versus values of selected environmental variables measured in the same sample. a) Thaumarchaeota rrs, b) Thaumarchaeota amoA, c) Thaumarchaeota ureC, d) Nitrospina rrs, e) [NH_4^+], f) [urea]. Samples from the WW are shown as Δ , samples from the CDW are shown as \square , and samples of SLOPE water are shown as X and red horizontal lines indicate the limits of detection for rate measurements. The significance of model 2 regressions of subsets of the data are given in Supplemental Table 7. Points CDW: 2060,17.8 and 179; SLOPE: 1756, 0.82 and 0.25 were omitted from panel "f" to improve the resolution of points near the origins.

Supplemental Figure 6. Oxidation rates of N supplied as urea (UO) versus values of selected environmental variables measured in the same sample. a) Thaumarchaeota *rrs*, b) Thaumarchaeota *amoA*, c) Thaumarchaeota *ureC*, d) *Nitrospina rrs*, e) [NH₄⁺], f) [urea], g) ratio ([urea-N]/[ammonium-N]), h) urea availability ([urea-N]/([urea-N] + [ammonium-N])). The significance of model 2 regressions of subsets of the data are given in Supplemental Table 7. Symbols as in Supplemental Figure 5. Some points have been omitted from the plots (see panels) to improve the resolution of points near the origins.

Supplemental Figure 7. Time courses of the production of ¹⁵NO_x from ¹⁵N-labeled NH₄⁺ and urea. Samples were collected at the stations and depths indicated, replicate 250 mL bottles were amended with ¹⁵N-labeled substrate, then incubated in the same incubator as survey measurements. Duplicate bottles were removed at the times shown, 40 mL was decanted from each bottle into a centrifuge tube and frozen at -80 °C until they could be analyzed for ¹⁵NO_x content. The slopes of time courses were determined using Pearson product moment regressions.

Supplemental Table 1. Data collected on cruise LMG1801. The two rows labeled "Measurement Precision" and "Limit of Detection" provide estimates of those values for the data in the columns below the entries. See text for details. Column headings give measurement names and units and are generally self-explanatory. Cells in the "Experimental Replicate" column containing the text "48 hr", "44 nM" and "T=0" are from experiments to verify our protocols (respectively: time courses, concentration dependence, and temperature dependence). Replicates simply labeled "A" and "B" are from survey measurements. Environmental and qPCR data for a given sample are listed with the "A" replicate of rate measurements, though they also apply to the "B" replicate. Otherwise, blank cells indicate no data. Outliers enclosed in parentheses have been excluded from calculations of descriptive statistics (presented in Supplemental Table 3) for the water mass in which they occur. Shading indicates water mass designation (ASW 0-34m; WW 35-174 m; CDW 175-1000 m; SLOPE 2500-3048 m).

Supplemental Table 2. Descriptive statistics of water mass properties and comparison with values from samples used to test experimental protocols. Sample means in columns at right are the means of all rate measurements made for that sample (station and depth, Supplemental Table 2), means that were less than the limit of detection (<LD) were excluded from further calculations. AO = oxidation of NH₄⁺, UO = oxidation of urea-N. Rows at the bottom of the table compare values of variables and parameters to water mass means. Values that are significantly different from the water mass mean (*t*-test, p<0.01) are indicated in *BOLD RED ITALICS*. Blank cells indicate no data for that variable or parameter. Shading highlights water mass designations.

Supplemental Table 3. Q_{10} and T_{min} values calculated from data in Figure 2. T_{min} values calculated as per (1).

Supplemental Table 4. Results of Mann Whitney ranks tests of the distribution of variables across the study area by sampling day and geographic location. Areal distributions of the data by water mass are shown in Supplemental Figure 3. The stations were assigned to subsets by sampling day ("Days 1-15" vs "Days 16-30") and geographic region ("Northeast" vs "Southwest" or "Inshore" vs "Offshore,"), see Supplemental Table 2 for assignments of individual stations to groups, then data from a given water mass were tested to determine if their distribution between subsets was random (H₀ is that there is no difference between subsets, rejected if p < 0.01, shown as **BOLD RED ITALICS**). Values given are the means of each subset followed by the probability that the distribution of values between subsets is random. One outlier from the CDW, offshore, urea data (2,060 nM) was excluded from calculations. We did not test the ASW or SLOPE data sets because most of the samples from those water masses were collected during the first half of the cruise (days 1-15). The SLOPE data sets are small ($n \le 16$, including duplicate measurements of the same sample), there were too few measurements of the abundance of some genes in ASW samples, and too many values of AO and UO rates in the ASW water mass were below the limit of detection, thus assigned vales of 0, for tests of spatial distributions within this water mass to be meaningful.

Supplemental Table 5. Results of Kruskal-Wallis ranks tests of the uniformity of the distribution of variables among water masses.

Supplemental Table 6. Summary of Model II, ordinary least squares regressions of variables related to the oxidation of N supplied as urea or ammonium in samples collected on LMG1801. n is the number of observations, r is the correlation coefficient, P is the probability that the slope $\neq 0$. *P*-values are for r and were derived from 999 bootstrap iterations. Rates <LD

were assigned values of 0 for the analyses. Ratios used means of rates measured in a given sample where both rates are >LD. AO – oxidation of ammonium N; UO – oxidation of urea N.

Supplemental Table 7. Contribution of urea-N relative to NH₄⁺ to nitrite production measured in other studies.

Supplemental Table 8. Primers and probes used in this study, qPCR cycling program, number of plates run, primer efficiencies and limits of detection.

Supplemental Table 9. Comparison of N oxidation rates from time courses of ¹⁵NO_x production with measurements from other experiments with the same sample. Rates were calculated from time courses as the slopes of Pearson product-moment regressions and are reported as "rate (R², lower 99% CL-upper 99% CL)." "Rates from 48 hr points" are calculated from samples taken at ~48 hours during time course incubations. "Rates from end-point determinations" are from incubations that were only sampled once after ~48 hr of incubation. "Survey" samples were from the survey of nitrification rates across the PAL LTER study area. "44 nM" are from samples amended with 44 nM of ¹⁵N-labeled substrate as part of a study of the response of nitrifiers to higher or lower substrate concentrations. "Temp = 0" samples were part of a study to assess the effect of incubation temperature on rates. "Rep A" and "Rep B" indicate separate independent incubations (replicates). "dup" indicates samples for which ¹⁵NO_x analyses were replicated. "ASW," Antarctic Surface Water, samples from 10-15 m; "WW," Winter Water, samples from the temperature minimum between 35-100 m; "CDW," Circumpolar Deep Water, 175-1000 m. Rates that are significantly different (99% CL) from rates determined by time course regressions are indicated by **BOLD RED ITALICS**.

LITERATURE CITED (1,743 words, 11,943 characters including spaces)

- 1. Ratkowsky DA, Olley J, McMeekin TA, Ball A. 1982. Relationship between temperature and growth rate of bacterial cultures. Journal of Bacteriology 149:1-5.
- van Gestel NC, Ducklow HW, Bååth E. 2020. Comparing temperature sensitivity of bacterial growth in Antarctic marine water and soil. Global Change Biology 26:2280-2291.
- 3. Konneke M, Bernhard AE, de la Torre JR, Walker CB, Waterbury JB, Stahl DA. 2005. Isolation of an autotrophic ammonia-oxidizing marine archaeon. Nature 437:543-546.
- 4. Prosser JI, Nicol GW. 2008. Relative contributions of archaea and bacteria to aerobic ammonia oxidation in the environment. Environmental Microbiology 10:2931-2941.
- 5. Ward BB, Arp DJ, Klotz MG. 2011. Nitrification. ASM Press, Washington, D.C.
- 6. DeLong EF, Wu KY, Prezelin BB, Jovine RVM. 1994. High abundance of Archaea in Antarctic marine picoplankton. Nature 371:695-697.
- 7. Massana R, Taylor LT, Murray AE, Wu KY, Jeffrey WH, DeLong EF. 1998. Vertical distribution and temporal variation of marine planktonic archaea in the Gerlache Strait, Antarctica, during early spring. Limnology and Oceanography 43:607-617.
- 8. Murray AE, Wu KY, Moyer CL, Karl DM, DeLong EF. 1999. Evidence for circumpolar distribution of planktonic Archaea in the Southern Ocean. Aquatic Microbial Ecology 18:263-273.
- 9. Hallam SJ, Konstantinidis KT, Putnam N, Schleper C, Watanabe Y-i, Sugahara J, Preston C, de la Torre J, Richardson PM, DeLong EF. 2006. Genomic analysis of the uncultivated marine crenarchaeote *Cenarchaeum symbiosum*. Proceedings of the National Academy of Sciences 103:18296-18301.

- Tourna M, Stieglmeier M, Spang A, Könneke M, Schintlmeister A, Urich T, Engel M,
 Schloter M, Wagner M, Richter A, Schleper C. 2011. Nitrososphaera viennensis, an
 ammonia oxidizing archaeon from soil. Proceedings of the National Academy of
 Sciences 108:8420-8425.
- 11. Qin W, Amin SA, Martens-Habbena W, Walker CB, Urakawa H, Devol AH, Ingalls AE, Moffett JW, Armbrust EV, Stahl DA. 2014. Marine ammonia-oxidizing archaeal isolates display obligate mixotrophy and wide ecotypic variation. Proceedings of the National Academy of Sciences 111:12504-12509.
- 12. Bayer B, Vojvoda J, Offre P, Alves RJE, Elisabeth NH, Garcia JAL, Volland J-M, Srivastava A, Schleper C, Herndl GJ. 2016. Physiological and genomic characterization of two novel marine thaumarchaeal strains indicates niche differentiation. ISME Journal 10:1051-1063.
- 13. Carini P, Dupont CL, Santoro AE. 2018. Patterns of thaumarchaeal gene expression in culture and diverse marine environments. Environmental Microbiology 20:2112-2124.
- 14. Alonso-Sáez L, Waller AS, Mende DR, Bakker K, Farnelid H, Yager PL, Lovejoy C, Tremblay J-É, Potvin M, Heinrich F, Estrada M, Riemann L, Bork P, Pedrós-Alió C, Bertilsson S. 2012. Role for urea in nitrification by polar marine Archaea. Proceedings of the National Academy of Sciences 109:17989-17994.
- 15. Pedneault E, Galand PE, Potvin M, Tremblay J-É, Lovejoy C. 2014. Archaeal amoA and ureC genes and their transcriptional activity in the Arctic Ocean. Scientific Reports 4:4661.

- 16. Wan XS, Sheng H-X, Dai M, Church MJ, Zou W, Li X, Hutchins DA, Ward BB, Kao S-J. 2021. Phytoplankton-Nitrifier Interactions Control the Geographic Distribution of Nitrite in the Upper Ocean. Global Biogeochemical Cycles 35:e2021GB007072.
- 17. Laperriere SM, Morando M, Capone DG, Gunderson T, Smith JM, Santoro AE. 2021.

 Nitrification and nitrous oxide dynamics in the Southern California Bight. Limnology and Oceanography 66:1099-1112.
- 18. Kitzinger K, Padilla CC, Marchant HK, Hach PF, Herbold CW, Kidane AT, Könneke M, Littmann S, Mooshammer M, Niggemann J, Petrov S, Richter A, Stewart FJ, Wagner M, Kuypers MMM, Bristow LA. 2019. Cyanate and urea are substrates for nitrification by Thaumarchaeota in the marine environment. Nature Microbiology 4:234-243.
- 19. Shiozaki T, Hashihama F, Endo H, Ijichi M, Takeda N, Makabe A, Fujiwara A, Nishino S, Harada N. 2021. Assimilation and oxidation of urea-derived nitrogen in the summer Arctic Ocean. Limnology and Oceanography 66:4159-4170.
- Tolar BB, Wallsgrove NJ, Popp BN, Hollibaugh JT. 2017. Oxidation of urea-derived nitrogen by thaumarchaeota-dominated marine nitrifying communities. Environmental Microbiology 19:4838-4850.
- 21. Martinson DG, Stammerjohn SE, Iannuzzi RA, Smith RC, Vernet M. 2008. Western Antarctic Peninsula physical oceanography and spatio–temporal variability. Deep Sea Research Part II: Topical Studies in Oceanography 55:1964-1987.
- 22. Church MJ, DeLong EF, Ducklow HW, Karner MB, Preston CM, Karl DM. 2003.
 Abundance and distribution of planktonic Archaea and Bacteria in the waters west of the Antarctic Peninsula. Limnology and Oceanography 48:1893-1902.

- 23. Baer SE, Sipler RE, Roberts QN, Yager PL, Frischer ME, Bronk DA. 2017. Seasonal nitrogen uptake and regeneration in the western coastal Arctic. Limnology and Oceanography 62:2463-2479.
- 24. Shiozaki T, Ijichi M, Isobe K, Hashihama F, Nakamura K-i, Ehama M, Hayashizaki K-i, Takahashi K, Hamasaki K, Furuya K. 2016. Nitrification and its influence on biogeochemical cycles from the equatorial Pacific to the Arctic Ocean. ISME J doi:10.1038/ismej.2016.18.
- 25. Ward BB, O'Mullan GD. 2005. 24. Community level analysis: genetic and biogeochemical approaches to investigate community composition and function in aerobic ammonia oxidation. , p 395-413, Methods in Enzymology, vol 397. Elsevier Inc., New York.
- 26. Kim J-G, Park S-J, Sinninghe Damsté JS, Schouten S, Rijpstra WIC, Jung M-Y, Kim S-J, Gwak J-H, Hong H, Si O-J, Lee S, Madsen EL, Rhee S-K. 2016. Hydrogen peroxide detoxification is a key mechanism for growth of ammonia-oxidizing archaea.
 Proceedings of the National Academy of Sciences 113:7888-7893.
- 27. Tolar BB, Powers LC, Miller WL, Wallsgrove NJ, Popp BN, Hollibaugh JT. 2016.
 Ammonia oxidation in the ocean can be inhibited by nanomolar concentrations of hydrogen peroxide. Frontiers in Marine Science 3.
- 28. Qin W, Meinhardt KA, Moffett JW, Devol AH, Virginia Armbrust E, Ingalls AE, Stahl DA. 2017. Influence of oxygen availability on the activities of ammonia-oxidizing archaea. Environmental Microbiology Reports doi:10.1111/1758-2229.12525:n/a-n/a.
- Murray AE, Preston CM, Massana R, Taylor LT, Blakis A, Wu K, DeLong EF. 1998.
 Seasonal and spatial variability of Bacterial and Archaeal assemblages in the coastal

- waters near Anvers Island, Antarctica. Applied and Environmental Microbiology 64:2585-2595.
- 30. Kalanetra KM, Bano N, Hollibaugh JT. 2009. Ammonia-oxidizing *Archaea* in the Arctic Ocean and Antarctic coastal waters. Environmental Microbiology 11:2434–2445.
- Tolar BB, Ross MJ, Wallsgrove NJ, Liu Q, Aluwihare LI, Popp BN, Hollibaugh JT.
 2016. Contribution of ammonia oxidation to chemoautotrophy in Antarctic coastal waters. ISME Journal 10:2605–2619.
- 32. Zinser ER, Coe A, Johnson ZI, Martiny AC, Fuller NJ, Scanlan DJ, Chisholm SW. 2006.
 Prochlorococcus ecotype abundances in the North Atlantic Ocean as revealed by ani
 mproved quantitative PCR method. Applied and Environmental Microbiology 72:723-732.
- 33. Hollibaugh JT. 2017. Oxygen and the activity and distribution of marine Thaumarchaeota. Environmental Microbiology Reports 9:186-188.
- 34. Resing J, Letelier RM, Karl DM. 1993. Palmer LTER: Hydrogen Peroxide in the Palmer LTER region: II Water column distribution. Antarctic Journal of the United States 1993:227-228.
- 35. Shanks AL, Trent JD. 1979. Marine snow: Microscale nutrient patches1. Limnology and Oceanography 24:850-854.
- 36. Alldredge AL, Silver MW. 1988. Characteristics, dynamics and significance of marine snow. Progress in Oceanography 20:41-82.
- 37. Baer SE, Connelly TL, Sipler RE, Yager PL, Bronk DA. 2014. Effect of temperature on rates of ammonium uptake and nitrification in the western coastal Arctic during winter, spring, and summer. Global Biogeochemical Cycles 28:1455-1466.

- 38. Hollibaugh JT, Wong PS, Azam F, Smith DC, Steward GF, Cole BE. 1992. Measurement of bacterioplankton production in Antarctic coastal waters: Comparison of thymidine and L-leucine methods and verification of labeling patterns. Antarctic Journal of the United States 27:127-128.
- Li WKW, Dickie PM. 1987. Temperature characteristics of photosynthetic and heterotrophic activities - seasonal variations in temperate microbial plankton. Applied and Environmental Microbiology 53:2282-2295.
- 40. Mosier AC, Francis CA. 2011. 9. Determining the distribution of marine and coastal ammonia-oxidizing Archaea and Bacteria using a quantitative approach. Methods in Enzymology 486:205-221.
- 41. Wuchter C, Abbas B, Coolen MJL, Herfort L, van Bleijswijk J, Timmers P, Strous M, Teira E, Herndl GJ, Middelburg JJ, Schouten S, Sinninghe Damste JS. 2006. Archaeal nitrification in the ocean. Proceedings of the National Academy of Sciences 103:12317-12322.
- 42. Suzuki MT, Taylor LT, DeLong EF. 2000. Quantitative analysis of small-subunit rRNA genes in mixed microbial populations via 5'-nuclease assays. Applied and Environmental Microbiology 66:4605-4614.
- 43. Kitzinger K, Marchant HK, Bristow LA, Herbold CW, Padilla CC, Kidane AT, Littmann S, Daims H, Pjevac P, Stewart FJ, Wagner M, Kuypers MMM. 2020. Single cell analyses reveal contrasting life strategies of the two main nitrifiers in the ocean. Nature Communications 11:767.
- 44. Pachiadaki MG, Sintes E, Bergauer K, Brown JM, Record NR, Swan BK, Mathyer ME, Hallam SJ, Lopez-Garcia P, Takaki Y, Nunoura T, Woyke T, Herndl GJ, Stepanauskas R.

- 2017. Major role of nitrite-oxidizing bacteria in dark ocean carbon fixation. Science 358:1046.
- 45. Widner B, Fuchsman CA, Chang BX, Rocap G, Mulholland MR. 2018. Utilization of urea and cyanate in waters overlying and within the eastern tropical north Pacific oxygen deficient zone. FEMS Microbiology Ecology 94.
- 46. Mincer TJ, Church MJ, Taylor LT, Preston C, Karl DM, DeLong EF. 2007. Quantitative distribution of presumptive archaeal and bacterial nitrifiers in Monterey Bay and the North Pacific Subtropical Gyre. Environmental Microbiology 9:1162-1175.
- 47. EPA. 2000. Practical Methods for Data Analysis Information OoE, US Environmental Protection Agency, Washington DC.
- 48. Koch H, Lücker S, Albertsen M, Kitzinger K, Herbold C, Spieck E, Nielsen PH, Wagner M, Daims H. 2015. Expanded metabolic versatility of ubiquitous nitrite-oxidizing bacteria from the genus Nitrospira. Proceedings of the National Academy of Sciences 112:11371–11376.
- 49. Holmes RM, Aminot A, Kerouel R, Hooker BA, Peterson BJ. 1999. A simple and precise method for measuring ammonium in marine and freshwater ecosystems. Canadian Journal of Fisheries and Aquatic Science 56:1801-1808.
- Santoro AE, Casciotti KL, Francis CA. 2010. Activity, abundance and diversity of nitrifying archaea and bacteria in the central California Current. Environmental Microbiology 12:1989–2006.
- 51. Beman JM, Chow C-E, King AL, Feng Y, Fuhrman JA, Andersson A, Bates NR, Popp BN, Hutchins DA. 2011. Global declines in oceanic nitrification rates as a consequence of ocean acidification. Proceedings of the National Academy of Sciences 108:208-213.

- 52. Sigman DM, Casciotti KL, Andreani M, Barford C, Galanter M, Bohlke JK. 2001. A bacterial method for the nitrogen isotopic analysis of nitrate in seawater and freshwater.

 Analytical Chemistry 73:4145-4153.
- 53. Popp BN, Sansone FJ, Rust TM, Merritt DA. 1995. Determination of concentration and carbon isotopic composition of dissolved methane in sediments and nearshore waters.
 Analytical Chemistry 67:405-411.
- 54. Dore JE, Popp BN, Karl DM, Sansone FJ. 1998. A large source of atmospheric nitrous oxide from subtropical North Pacific surface waters. Nature 396:63-66.
- 55. Casciotti KL, Sigman DM, Hastings MG, Böhlke JK, Hilkert A. 2002. Measurement of the oxygen isotopic composition of nitrate in seawater and freshwater using the denitrifier method. Analytical Chemistry 74:4905-4912.
- 56. Legendre P. 2001. Model II regression User's guide. Département de sciences biologiques, Université de Montréal, Montreal, Quebec, Canada.